Calcium sparks and excitation–contraction coupling in phospholamban-deficient mouse ventricular myocytes

L. F. Santana *, E. G. Kranias † and W. J. Lederer *

** Department of Molecular Biology and Biophysics, Medical Biotechnology Center, University of Maryland Biotechnology Institute and Department of Physiology, University of Maryland at Baltimore School of Medicine, 725 West Lombard Street, Baltimore, MD 21201 and † Department of Pharmacology and Cell Biophysics, University of Cincinnati, PO Box 670575, Cincinnati, OH 45267-0575, USA*

1. We examined $[Ca^{2+}]_i$ and L-type Ca^{2+} channel current (I_{Ca}) in single cardiac myocytes to determine how the intracellular protein phospholamban (PLB) influences excitation–contraction (E–C) coupling in heart. Wild type (WT) and PLB-deficient (KO) mice were used. Cells were patch clamped in whole-cell mode while $[Ca^{2+}]_i$ was imaged simultaneously using the Ca^{2+} indicator fluo-3 and a confocal microscope.

2. Although I_{Ca} was similar in magnitude, the decay of I_{Ca} was faster in KO than in WT cells and the $[Ca^{2+}]_i$ transient was larger and decayed faster. Furthermore, the E–C coupling 'gain' (measured as $\Delta[Ca^{2+}]_i/I_{Ca}$) was larger in KO cells than in WT cells.

3. Spontaneous Ca^{2+} sparks were three times more frequent and larger in KO cells than in WT myocytes but, surprisingly, the time constants of decay were similar.

4. SR Ca^{2+} content was significantly greater in KO than in WT cells. When the SR Ca^{2+} content in KO cells was reduced to that in WT cells, Ca^{2+} sparks in these 'modified' (KO′) cells decayed faster. E–C coupling gain, $[Ca^{2+}]_i$ transient amplitude and the kinetics of decay of I_{Ca} were similar in KO′ and WT cells.

5. We conclude that SR Ca^{2+} content influences (1) I_{Ca}, (2) the amplitude and kinetics of Ca^{2+} sparks and $[Ca^{2+}]_i$ transients, (3) the sensitivity of the RyRs to triggering by $[Ca^{2+}]_i$, (4) the amount of Ca^{2+} released, (5) the magnitude of the E–C coupling 'gain' function, and (6) the rate of Ca^{2+} re-uptake by the SR Ca^{2+}-ATPase. In KO cells, the larger $[Ca^{2+}]_i$ transients and Ca^{2+} sparks speed up I_{Ca} inactivation. Finally, we conclude that PLB plays an important regulatory role in E–C coupling by modulating SR Ca^{2+}-ATPase activity, which establishes the SR Ca^{2+} content and consequently influences the characteristics of local and global Ca^{2+} signalling.

During excitation–contraction (E–C) coupling, voltage-gated L-type Ca^{2+} channels, identified as dihydropyridine receptors (DHPRs), open briefly so that each allows the influx of a small amount of Ca^{2+} into the cardiac myoplasm. The Ca^{2+} influx through an open Ca^{2+} channel is responsible for the stochastic activation of nearby RyRs located in the adjacent junctional SR by the mechanism of calcium-induced calcium release (CICR; Fabiato, 1983; Niggli & Lederer, 1990; Cannell, Cheng & Lederer, 1994; Cannell, Cheng & Lederer, 1995; López-López, Shacklock, Balke & Wier, 1995). The release of Ca^{2+} arising from the opening of a single RyR, or a few acting in concert, can be seen using a confocal microscope in cells loaded with the Ca^{2+}-sensitive indicator fluo-3 (Cheng, Lederer & Cannell, 1993). These elementary SR Ca^{2+} release events, called 'Ca^{2+} sparks', amplify the triggering signal from I_{Ca} and cause a rapid increase in cellular or 'global' $[Ca^{2+}]_i$ as the Ca^{2+} sparks sum to produce the $[Ca^{2+}]_i$ transient (Cannell *et al.* 1994, 1995). As I_{Ca} inactivates and as the cell repolarizes, fewer Ca^{2+} sparks are activated and the $[Ca^{2+}]_i$ transient declines so that pre-excitation conditions are restored (Cannell *et al.* 1995). $[Ca^{2+}]_i$ returns to resting levels due to the concerted actions of the SR Ca^{2+}-ATPase and the sarcolemmal Na^+–Ca^{2+} exchanger (Crespo, Grantham & Cannell, 1990; Balke, Egan & Wier, 1994). Phospholamban (PLB) is the protein that is the dominant regulator of the SR Ca^{2+}-ATPase (Lindemann, Jones, Hathaway, Henry & Watanabe, 1983). The specific influence that PLB has on contraction and E–C coupling has been suggested in previous reports (Luo *et al.* 1994; Kiss, Ball, Kranias & Walsh, 1995; Luo *et al.* 1996; Wolska, Stojanovic, Luo, Kranias & Solaro, 1996) but subcellular mechanisms and molecular controls of these mechanisms have not been elucidated.

PLB constitutively inhibits the SR Ca^{2+}-ATPase unless PLB is phosphorylated (Hicks, Shigekawa & Katz, 1979). There are two phosphorylation sites on PLB which are targets for protein kinase A (PKA) and Ca^{2+}-calmodulin-dependent protein kinase (Ca^{2+}-calmodulin PK) (Simmerman, Collins, Theibert, Wegener & Jones, 1986). β-Adrenergic receptor activation leads to the phosphorylation of both of these sites on PLB and relieves its inhibitory actions on the SR Ca^{2+}-ATPase (by de-repressing it; Wegener, Simmerman, Lindemann & Jones, 1989; Talosi, Edes & Kranias, 1993). Activation of the Ca^{2+}-ATPase speeds up the re-uptake of Ca^{2+} into the SR, shortens the $[Ca^{2+}]_i$ transient and reduces the Ca^{2+} spark duration (Gómez, Cheng, Lederer & Bers, 1996) just as inhibition of the Ca^{2+}-ATPase by thapsigargin slows the $[Ca^{2+}]_i$ transient (Kirby, Sagara, Gaa, Inesi, Lederer & Rogers, 1992) and increases Ca^{2+} spark duration (Gómez *et al.* 1996). Using PKA or Ca^{2+}–calmodulin PK activation to study the actions of PLB is virtually impossible at the cellular level because there are multiple targets of PKA (e.g. RyRs, DHPRs, PLB), almost all of which affect E–C coupling and cellular function. We have taken advantage of the newly developed PLB 'knockout' mouse model (Luo *et al.* 1994) to examine the role of PLB in E–C coupling at the cellular and subcellular level and investigate the molecular basis of any altered function. A preliminary report of this work has been made to the Biophysical Society (Santana, Shioya, Kranias & Lederer, 1997).

METHODS

Cell isolation and electrophysiology

Hearts were obtained from adult (22–32 g) KO and WT mice killed by intraperitoneal injection of a lethal dose of pentobarbitone (100 mg kg^{-1}). Single mouse ventricular myocytes were isolated following the procedure of Powell, Noma, Shioya & Kozlowski (1993) for guinea-pig and stored at room temperature (22–25 °C) in Dulbecco's modified Eagle's medium (JRH Biosciences, Lanexa, KS, USA) until use (0·5–6 h after isolation). Membrane currents were measured using the whole-cell configuration of the patch-clamp technique with an Axopatch-200A amplifier (Axon Instruments). Patch pipettes were pulled with a Flaming Brown-type puller (Sutter Instrument Co., Novato, CA, USA) to a nominal resistance of 1–3 MΩ and filled with an internal solution of the following composition (mM): 130 CsCl, 5 MgATP, 10 Hepes, 20 TEA-Cl, and 0·1 fluo-3.

During experiments cells were continuously superfused with a normal Tyrode (NT) solution composed of (mM): 140 NaCl, 0·5 $MgCl_2$, 0·33 NaH_2PO_4, 5 Hepes, 5·5 glucose, 1·8 $CaCl_2$ and 5 KCl; pH 7·4, at a temperature of 34–37 °C. After successful conversion to the whole-cell configuration of the patch-clamp technique the external solution was changed to a modified NT solution (Cs-NT) designed to block K^+ currents and isolate I_{Ca} by substituting (1 : 1) CsCl for KCl. For the duration of the experiments cells were held at −80 mV. To ensure that steady-state loading of the SR Ca^{2+} was attained, four depolarizing pulses (1 Hz) of 50 ms duration to 0 mV were applied before the cell was depolarized to a given test potential using the following protocol. Five hundred milliseconds after the fourth conditioning pulse, cells were depolarized to −40 mV slowly (1 mV every 12·5 ms) and held at this potential for 50 ms (to inactivate Na^+ current) before rapid (step) depolarization to a test potential. All electrophysiological signals were analysed using pCLAMP 6.01 software (Axon Instruments).

Confocal microscopy

Cells were loaded with the fluorescent Ca^{2+}-sensitive indicator fluo-3 (potassium salt) through the patch pipette. Fluorescence images were collected using a Biorad MRC 600 (Cambridge, MA, USA) laser scanning confocal microscope (LSCM) equipped with a Zeiss Neofluor ×63 oil immersion lens (NA = 1·25). The LSCM was operated using a PC (Compaq) running SOM and COMOS software (Biorad, Cambridge, MA, USA). Images were analysed on an IBM-compatible PC running IDL software (Research Systems, Boulder, CO, USA). For analysis, images were normalized by dividing the fluorescence intensity of each pixel (F) by the average resting fluorescence intensity (F_0) of a confocal image to generate an F/F_0 image. The calibration of fluorescence signals was possible using the pseudoratio method (Cannell *et al.* 1994) because KO and WT diastolic $[Ca^{2+}]_i$ is known and is similar (Wolska *et al.* 1996).

Measurement of SR Ca^{2+} load

We used caffeine to estimate the SR Ca^{2+} load (Bassani, Yuan & Bers, 1995) and the amplitude of a caffeine-induced $[Ca^{2+}]_i$ transient was then used as an index of the amount of Ca^{2+} stored in the SR. In these experiments, a sodium- and calcium-free Tyrode solution was used to superfuse the cell under investigation to eliminate Ca^{2+} extrusion or entry by the Na^+–Ca^{2+} exchanger. To this solution 20 mM caffeine was added and the solution was rapidly applied after a series of four depolarizing pulses (0·5 Hz) to 0 mV (50 ms) were given.

In some experiments the load of Ca^{2+} in the SR of KO cells was reduced to match that of WT myocytes by an experimental protocol that involved a series of steps. KO ventricular myocytes were first depolarized four times to 0 mV for 50 ms and then exposed to a caffeine solution. This first caffeine application depleted the SR of Ca^{2+} and provided an estimate of the initial SR Ca^{2+} content. After the first caffeine-induced $[Ca^{2+}]_i$ transient was recorded, cells were returned to a Cs-NT solution and depolarized six times for 50 ms to 0 mV to refill the SR of KO cells with Ca^{2+} to a level similar to that of WT cells (see Results). After this protocol, KO cells had an SR Ca^{2+} load similar to WT cells and are called KO′ cells. Experiments on these KO′ cells were then carried out as described in the text. To verify that the SR Ca^{2+} content in KO′ cells was similar to that in WT cells, a second exposure to the caffeine solution was carried out during the experiment.

Statistical analysis

Data are presented as means ± standard error of the mean (S.E.M.). Two-sample comparisons were performed using Student's t test while multigroup comparisons were made using a one-way ANOVA and Tukey's test (Zar, 1984). In all statistical tests a $P < 0·05$ was used as a measure of statistical significance.

RESULTS

Kinetics and amplitudes of I_{Ca} and the $[Ca^{2+}]_i$ transient

Figure 1*A* shows two representative line-scan images obtained from WT and KO mouse ventricular myocytes during a 50 ms depolarization to 0 mV. The $[Ca^{2+}]_i$ transients are clearly larger and faster in KO cells than in WT cells in this representative result. The larger and faster $[Ca^{2+}]_i$

transient is consistent with a recent report (Wolska *et al.* 1996) using KO cardiac myocytes. However, this earlier result (Wolska *et al.* 1996) could have been complicated by alterations in the action potential (AP) shape or because of difficulties associated with using fura-2 AM to measure $[Ca^{2+}]_i$ (Berlin & Konishi, 1993).

We avoided the complications of using AM indicators and of having uncertain AP shape by using the patch-clamp method in the whole-cell mode and fluo-3 (potassium salt) to examine the $[Ca^{2+}]_i$ transient and I_{Ca} over a wide range of voltages. Interestingly, we found that the alterations in amplitude and kinetics of the $[Ca^{2+}]_i$ transient observed in KO cells were voltage dependent as shown in Fig. 1*B–D*. To investigate the origin of these effects in KO mouse cells, we examined I_{Ca} simultaneously, since it is responsible for triggering SR Ca^{2+} release (Cheng, Cannell & Lederer, 1994; Cannell *et al.* 1995; Santana, Cheng, Gómez, Cannell & Lederer, 1996). We found, however, that the peak I_{Ca} (pA pF^{-1}) magnitude was similar in KO ($n = 18$) and WT cells ($n = 18$; $P > 0{\cdot}05$).

Interestingly, we found that KO and WT cells had I_{Ca} with different kinetics. The data shows that in KO cells I_{Ca} decays faster than it does in WT cells (see Fig. 1*A–D*). It is well established that I_{Ca} declines with two time constants, inactivating as a result of both a Ca^{2+}-dependent and voltage-dependent processes (McDonald, Pelzer, Trautwein & Pelzer, 1994). The faster decay of I_{Ca} in KO cells shown in Fig. 1*B* can be largely accounted for by the faster first component. Note, however, that the magnitude of both components remains about the same for KO and WT cells (KO cells: $\tau_{fast} = 8{\cdot}68 \pm 0{\cdot}33$ ms, $A_{fast} = -8{\cdot}37 \pm 1{\cdot}52$ pA pF^{-1}, $\tau_{slow} = 19{\cdot}78 \pm 3{\cdot}04$ ms, $A_{slow} = -3{\cdot}04 \pm 0{\cdot}59$ pA pF^{-1}; $n = 18$; WT cells: $\tau_{fast} = 12{\cdot}28 \pm 1{\cdot}29$ ms, $A_{fast} = -9{\cdot}45 \pm 1{\cdot}19$ pA pF^{-1}, $\tau_{slow} = 22{\cdot}47 \pm 1{\cdot}89$ ms, $A_{slow} = -4{\cdot}11 \pm 0{\cdot}86$ pA pF^{-1}; $n = 18$). A_{fast} is the amplitude of the first component and τ_{fast} is the exponential time constant of decay while A_{slow} and τ_{slow} are the amplitude and exponential time constant of decay of the second or slower component. The faster decay of I_{Ca} in KO cells could be due to the loss of PLB *per se* or be an indirect result of that loss. The parallel alterations in the $[Ca^{2+}]_i$ transient and I_{Ca}, however, suggested to us that it may be helpful to examine the relationship between the two.

E–C coupling 'gain' and the sensitivity of SR Ca^{2+} release in KO and WT cells

Figure 1*E* shows how the E–C coupling 'gain function' (Santana *et al.* 1996) is larger in KO than in WT cells. This function, which estimates how the $[Ca^{2+}]_i$ transient depends on I_{Ca} at different voltages, is increased at all potentials and only approaches zero as I_{Ca}, the triggering event, approaches zero. The experiments presented in this paper, like those of Santana *et al.* (1996), were carried out at zero $[Na^+]_i$ to prevent the Na^+–Ca^{2+} exchanger from possibly triggering SR Ca^{2+} release (Leblanc & Hume, 1990; Levi, Spitzer, Kohmoto & Bridge, 1994; Lipp & Niggli, 1994; Grantham & Cannell, 1996). The dependence of the $[Ca^{2+}]_i$ transient on I_{Ca} is plotted in Fig. 1*F*. Thus, taken together the data in Fig. 1 suggest that the SR Ca^{2+} release process is 'more sensitive' to trigger Ca^{2+} at all potentials and that this is associated with altered (more rapid) kinetics of both I_{Ca} and the $[Ca^{2+}]_i$ transient. In the next series of experiments we investigated whether alteration in the properties of the elementary SR Ca^{2+} release events could be responsible for these kinetic changes.

Ca^{2+} sparks in WT and PLB knockout ventricular myocytes

To explain the more rapid $[Ca^{2+}]_i$ transients, since both time to peak (Fig. 1*B*) and the τ_{decay} of the $[Ca^{2+}]_i$ transient are decreased in KO cells (Fig. 1*D*), we examined the properties of the elementary SR Ca^{2+} release event, the Ca^{2+} spark. Figure 2*A* shows representative line-scan images of spontaneous Ca^{2+} sparks in WT and KO cells obtained at the resting potential of −80 mV. At this potential the spontaneous occurrence of Ca^{2+} sparks does not depend on triggering by the opening of DHPRs (Cheng *et al.* 1993; Cannell *et al.* 1995), but instead depends on ambient $[Ca^{2+}]_i$ and the 'sensitivity' of the RyRs (see Cheng, Lederer, Lederer & Cannell, 1996). We found that the spontaneous rate of Ca^{2+} spark occurrence is increased about 3-fold from $0{\cdot}88 \pm 0{\cdot}2$ sparks s^{-1} $(100\ \mu m)^{-1}$ in WT cells ($n = 12$ cells) to $2{\cdot}41 \pm 0{\cdot}67$ sparks s^{-1} $(100\ \mu m)^{-1}$ in KO cells ($n = 12$ cells) as shown in Fig. 2*B*. Since $[Ca^{2+}]_i$ is unchanged in KO cells (Wolska *et al.* 1996) this increase in Ca^{2+} spark rate indicates there is an increase sensitivity of the RyRs to triggering by $[Ca^{2+}]_i$ and this may account for the increase in E–C coupling gain and the larger $[Ca^{2+}]_i$ transient observed in KO cells.

The other properties of the Ca^{2+} sparks in WT and KO cells are shown in Fig. 2*C–F* and they reveal that the overall shape of the Ca^{2+} spark is similar in WT and KO cells (Fig. 2*C* and *D*) although the peak level is significantly higher in KO cells ($1{\cdot}89 \pm 0{\cdot}02$; peak $[Ca^{2+}]_i = 243 \pm 1{\cdot}6$ nM; $n = 117$) than in WT cells ($1{\cdot}65 \pm 0{\cdot}02$; peak $[Ca^{2+}]_i = 197 \pm 1{\cdot}6$ nM; $n = 116$; $P < 0{\cdot}05$). However, from our earlier study (Gómez *et al.* 1996), we had anticipated that Ca^{2+} sparks would decay more quickly in KO cells since we had shown that increases in the SR Ca^{2+}-ATPase activity increased the rate of decay of Ca^{2+} sparks. Here the rate of decay is similar in WT cells ($\tau_{decay} = 23{\cdot}67 \pm 1{\cdot}27$ ms; $n = 116$) and KO cells ($\tau_{decay} = 23{\cdot}91 \pm 1{\cdot}31$ ms; $n = 117$).

Effects of SR Ca^{2+} load on the kinetics of Ca^{2+} sparks

Because SR Ca^{2+} load has been shown to alter the properties of Ca^{2+} sparks, including peak level of $[Ca^{2+}]_i$ (increased), spatial size (increased), time constant of decay (increased) and frequency (increased) (Cheng *et al.* 1996), and because electron probe microanalysis has shown that Ca^{2+} in the junctional SR is greater in KO hearts than in WT hearts (Chu *et al.* 1996), we hypothesized that an increased SR Ca^{2+} load could contribute to the effects we observed in single cells. First, we used caffeine to estimate relative SR

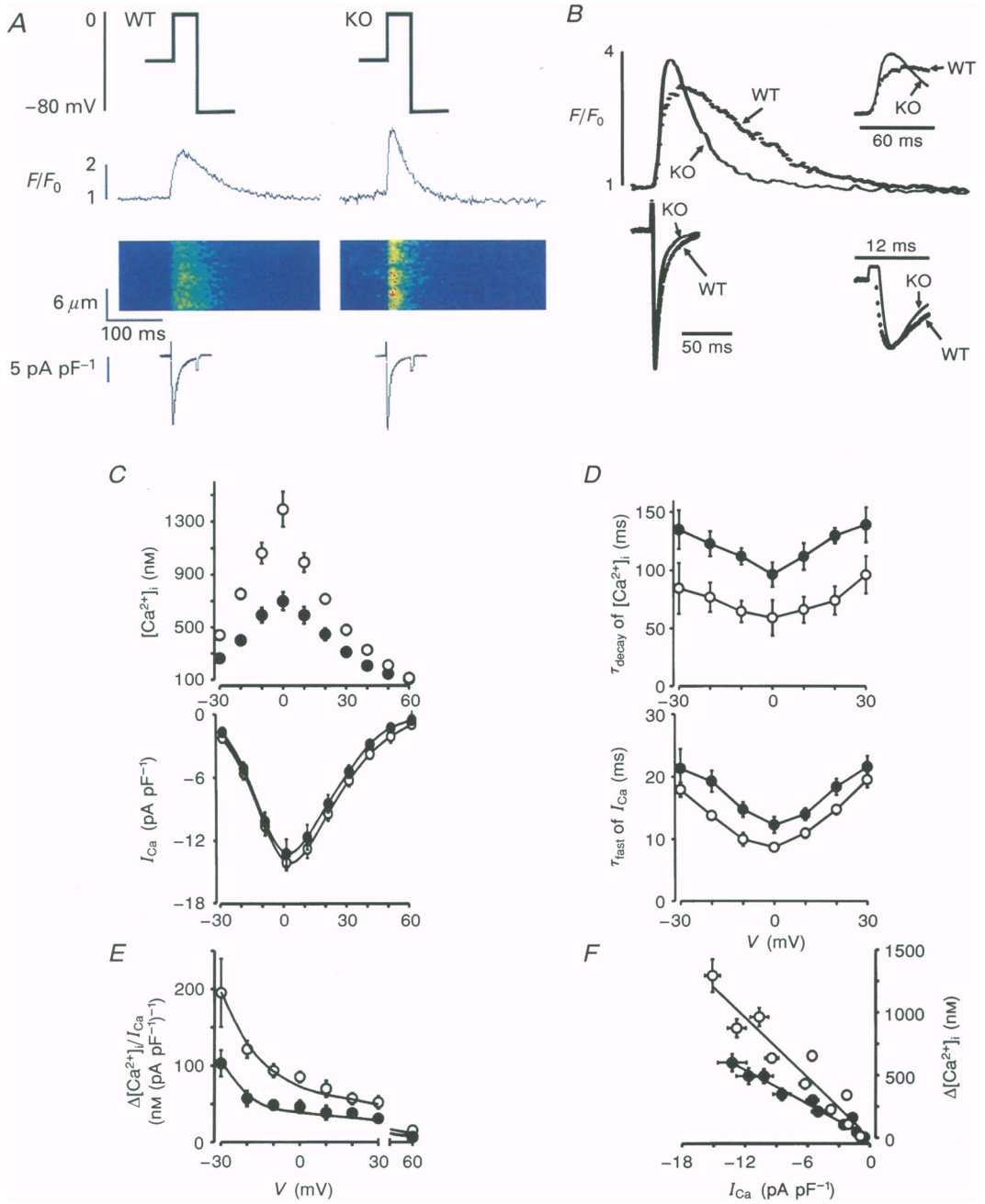

Figure 1. E–C coupling in WT and KO ventricular myocytes

A, representative line-scan images taken from WT and KO ventricular myocytes during a 50 ms depolarization to 0 mV. The upper section of this panel shows the voltage protocol employed for the acquisition of these images. The traces shown above the line-scan images represent the time course of the spatially averaged $[Ca^{2+}]_i$ transient. Under each image the simultaneously recorded I_{Ca} traces are shown. *B*, comparison of the time course of global $[Ca^{2+}]_i$ transients (top) and I_{Ca} (bottom) in WT (●) and KO (continuous line) ventricular myocytes. I_{Ca} current records were normalized to their peak values (I_{Ca} and $[Ca^{2+}]_i$ traces were simultaneously recorded). The insets shown at the right of each plot in this panel are enlarged views of the first portions of the I_{Ca} and $[Ca^{2+}]_i$ traces. *C*, voltage dependence of cell-wide $[Ca^{2+}]_i$ transients (top) and I_{Ca} (bottom) in WT (●; $n = 18$ cells from 6 animals) and KO (○; $n = 18$ cells from 8 animals) ventricular myocytes. *D*, voltage dependence of the rate of decay (τ_{decay}) of the global $[Ca^{2+}]_i$ transient (top) and I_{Ca} (bottom). The decaying phase of I_{Ca} was fitted with a two-exponential function using a least squares routine from which the first time constant (τ_{fast}) of the best fit function was used to construct this figure. *E*, voltage dependence of E–C coupling gain in WT (●) and KO (○) myocytes. The E–C coupling gain is expressed as the $\Delta[Ca^{2+}]_i$ (equal to the peak of the $[Ca^{2+}]_i$) transient minus the resting $[Ca^{2+}]_i$ which was assumed to be 100 nM (Wolska *et al.* 1996)) divided by the peak I_{Ca}. *F*, peak change in $[Ca^{2+}]_i$ as a function of peak I_{Ca} in WT (●) and KO (○) ventricular myocytes. Continuous lines are linear regression fits to the data (WT: $r^2 = 0{\cdot}96$, slope = −43·38 nM (pA pF^{-1})$^{-1}$; KO: $r^2 = 0{\cdot}90$, slope = −79·27 nM (pA pF^{-1})$^{-1}$.

Ca^{2+} content (see Methods). Figure 3*A* reveals that KO cells ($F/F_0 = 4{\cdot}12 \pm 0{\cdot}22$; $[Ca^{2+}]_i = 2050 \pm 255$ nM, $n = 10$) have significantly more SR Ca^{2+} than WT cells do ($F/F_0 = 3{\cdot}49 \pm 0{\cdot}14$; $[Ca^{2+}]_i = 954 \pm 150$ nM, $n = 6$; $P < 0{\cdot}05$). In order to assess the effects of SR Ca^{2+} load on the $[Ca^{2+}]_i$ transient, I_{Ca} and Ca^{2+} sparks, we used a protocol to reduce the SR Ca^{2+} load in KO cells (see Methods) to that of WT cells; we refer to them as KO′ cells ($F/F_0 = 3{\cdot}43 \pm 0{\cdot}25$; $[Ca^{2+}]_i = 934 \pm 62$ nM, $n = 4$; Fig. 3*A*). The remaining panels of Fig. 3 reveal how KO′ cells compare with WT cells. Figure 3*B–C* shows that when the magnitude of the $[Ca^{2+}]_i$ transient is reduced in the KO′ cells to that of WT cells, I_{Ca} peak levels remain unchanged in KO′ cells (but I_{Ca} peaks in KO and WT are also similar). More importantly, the E–C coupling gain in KO′ cells is similar to that in WT cells (Fig. 3*D*). Furthermore, reducing SR Ca^{2+} load in KO cells has a significant effect on the kinetics of I_{Ca} and $[Ca^{2+}]_i$ transients. First, $[Ca^{2+}]_i$ transients in KO′ cells have longer time-to-peak values ($32{\cdot}33 \pm 3{\cdot}15$ ms, $n = 4$) than those in KO cells ($15{\cdot}56 \pm 2{\cdot}58$; $n = 18$) but similar to those in WT

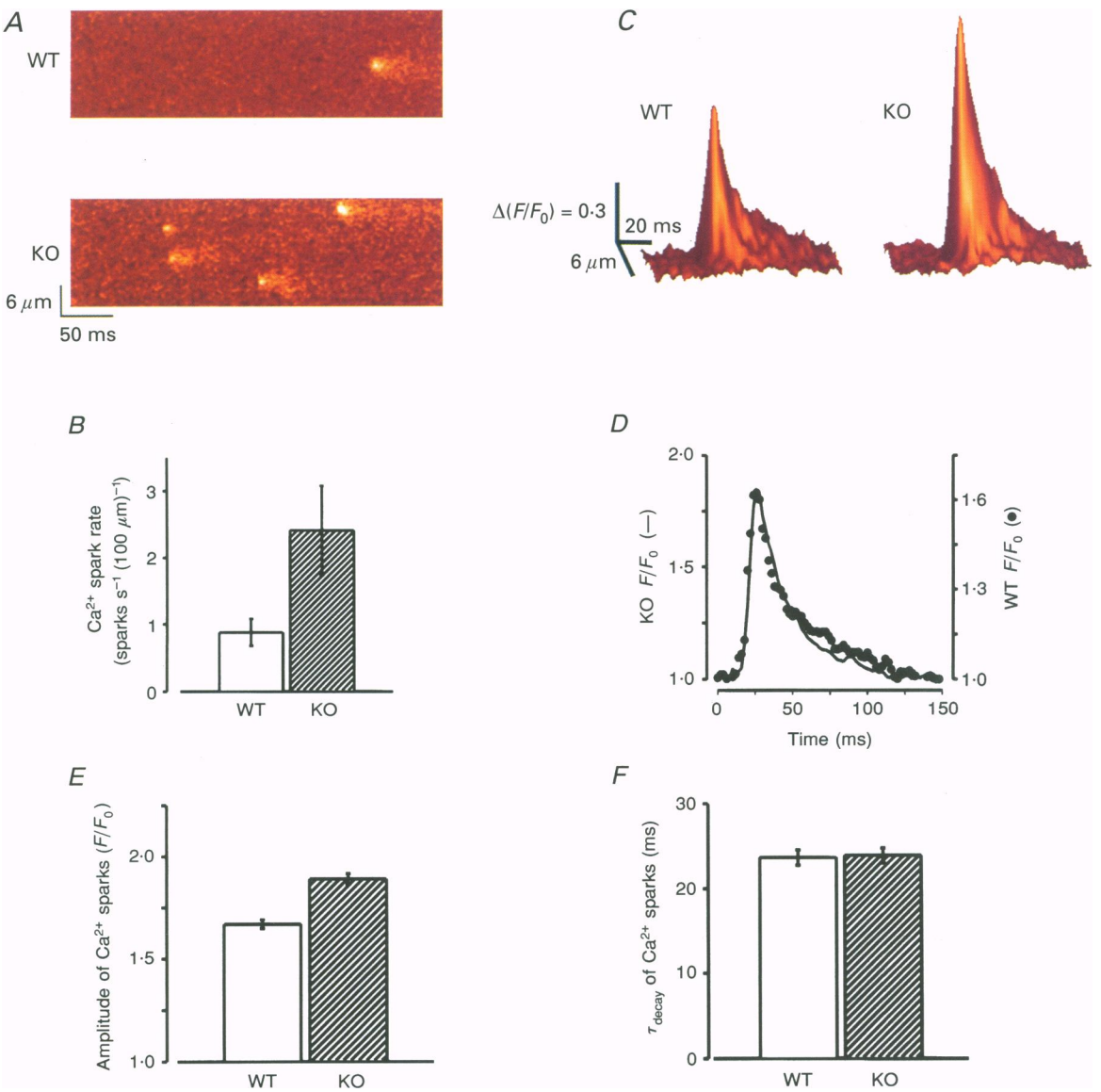

Figure 2. Properties of spontaneous Ca^{2+} sparks in WT and KO ventricular myocytes

A, representative line-scan images from WT (top) and KO (bottom) ventricular myocytes. These line-scan images were collected at a holding potential of −80 mV. *B*, rate of spontaneous Ca^{2+} spark occurrence in WT ($n = 12$ cells from 7 animals) and KO ($n = 12$ cells from 4 animals) ventricular cells. *C*, surface plot of averaged Ca^{2+} sparks from WT (left; $n = 116$ Ca^{2+} sparks from 7 animals) and KO myocytes (right; $n = 117$ Ca^{2+} sparks from 4 animals). The vertical scale bar in *C* represents a fluorescence change of 0·3 in F/F_0, where baseline $F/F_0 = 1$. *D*, time course of the averaged WT (●) and KO (continuous line) Ca^{2+} sparks shown in *C*. *E*, amplitude of spontaneous Ca^{2+} sparks in WT and KO ventricular myocytes. *F*, time constant of decay (τ_{decay}) of Ca^{2+} sparks in WT and KO cells.

cells ($30{\cdot}86 \pm 2{\cdot}44$ ms, $n = 18$). This suggest that I_{Ca} triggers SR Ca^{2+} release in a similar manner in KO′ and in WT cells. Nevertheless, there should be clear evidence that in KO′ cells the Ca^{2+}-ATPase is still able to remove cytosolic Ca^{2+} more rapidly than in WT cells. Indeed, the τ_{decay} of the $[Ca^{2+}]_i$ transient of KO′ cells is still faster than in WT ventricular myocytes (Fig. 3*E*). Note also that the rate of decline is faster at all potentials in KO′ cells than in KO cells, suggesting that an increased SR Ca^{2+} content slows down the net pumping rate of the Ca^{2+}-ATPase. Finally, the τ_{fast} of I_{Ca} is similar in KO′ and WT cells suggesting that by reducing SR Ca^{2+} load we may be reducing local SR Ca^{2+} release, which then inactivates I_{Ca} less quickly. To test this possibility we examined Ca^{2+} sparks in KO′ cells (Fig. 4). While the peak levels of local $[Ca^{2+}]_i$ are similar in KO′ cells ($1{\cdot}70 \pm 0{\cdot}05$; peak $[Ca^{2+}]_i = 206{\cdot}06 \pm 4{\cdot}04$ nM, $n = 39$) and WT cells ($1{\cdot}65 \pm 0{\cdot}02$; peak $[Ca^{2+}]_i = 197 \pm 1{\cdot}6$ nM; $n = 116$; Fig. 4*A–B*), the rate of decay of local $[Ca^{2+}]_i$ in a Ca^{2+} spark is faster in KO′ than in WT cells (Fig. 4*C*). In brief, many of the features of Ca^{2+} signalling in KO′ cells are similar to those seen in WT cells. I_{Ca}, the $[Ca^{2+}]_i$ transient, and Ca^{2+} sparks are similar in magnitude in WT and KO′ cells. In KO′ cells, however, the Ca^{2+} spark decays ($\tau_{decay} = 18{\cdot}56 \pm 1{\cdot}63$ ms, $n = 39$) more rapidly than in WT cells ($\tau_{decay} = 23{\cdot}67 \pm 1{\cdot}27$ ms, $n = 116$; $P < 0{\cdot}05$). Furthermore, in KO′ cells the global $[Ca^{2+}]_i$ transient decays more quickly than in the WT cells, and also more quickly than in KO cells.

DISCUSSION

The control of E–C coupling in heart depends on many proteins that control and respond to the $[Ca^{2+}]_i$ transient. In the mammalian heart PLB has been suggested to be one of these important regulatory proteins (Luo *et al.* 1994; Luo *et al.* 1996; Wolska *et al.* 1996). To investigate the actions of PLB in E–C coupling we have used a newly developed animal model (i.e. the KO mouse) that has been genetically developed to have no functional PLB gene and thus the animal makes no PLB (Luo *et al.* 1994).

In the KO mouse heart cells the effects of removing PLB from the heart may depend to a great extent on the increase in SR Ca^{2+} content due to the enhanced SR Ca^{2+}-ATPase activity. The two direct effects that are unmasked by reducing the SR Ca^{2+} content in the KO cells to that in WT cells (i.e. the KO′ cells) are the effect of Ca^{2+} pumping by the SR Ca^{2+}-ATPase on the Ca^{2+} spark rate of decline (fastest in KO′ cells) and on the rate of decline of the cellular $[Ca^{2+}]_i$ transient (faster in KO′ cells). Other prominent alterations in Ca^{2+} signalling seen in KO cells, such as the increased strength of contraction in the KO cells (Wolska *et al.* 1996), or the larger $[Ca^{2+}]_i$ transient that rises more quickly, disappear when SR Ca^{2+} content of the KO cell is made equal to that of the WT cell. The augmented E–C coupling gain (i.e. the increased sensitivity of the RyRs to triggering by local $[Ca^{2+}]_i$) that we have shown to be present in KO cells is absent when SR Ca^{2+} content of the KO cells is equal

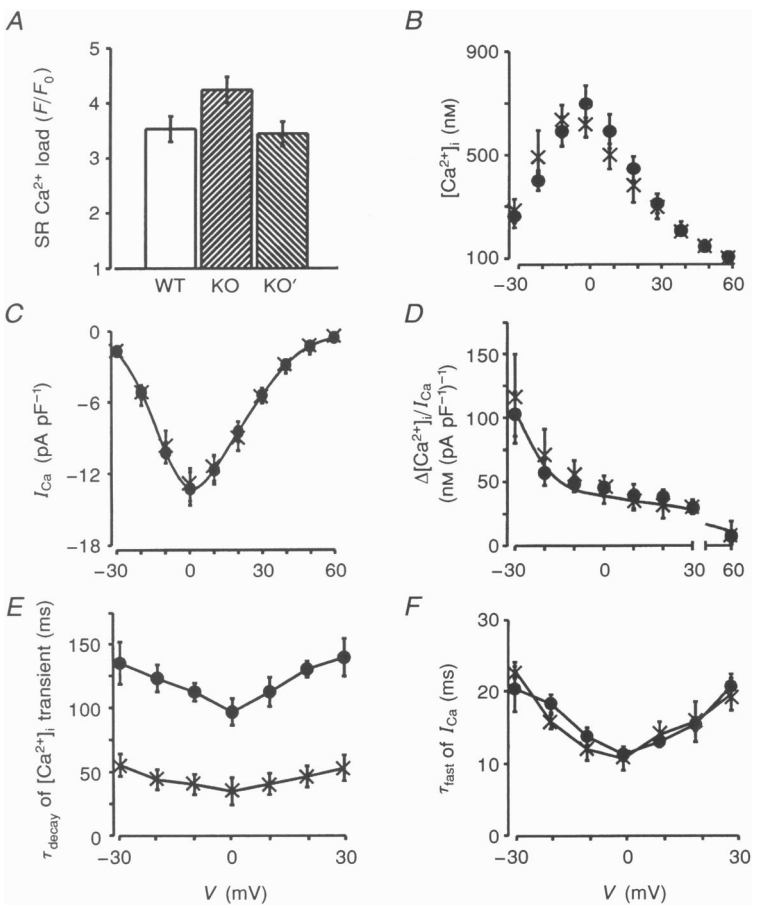

Figure 3. Effects of SR Ca^{2+} load in E–C coupling

A, SR Ca^{2+} load in WT ($n = 6$ cells from 3 animals), KO ($n = 10$ cells from 7 animals) and KO cells modified to have an SR Ca^{2+} load similar to that of WT cells (see Methods), called KO′ ventricular myocytes ($n = 4$ cells from 3 animals). *B–F* show the voltage dependence of the global $[Ca^{2+}]_i$ transient (*B*), I_{Ca} (*C*), E–C coupling gain (*D*), time constant of decay (τ_{decay}) of the global $[Ca^{2+}]_i$ transient (*E*), and fast time constant of decay (τ_{fast}) of I_{Ca} (*F*) in WT (●) and KO′ (×) ventricular myocytes. WT data shown in *B–F* of this figure are taken from Fig. 1.

to that of the WT myocytes. The more frequent Ca^{2+} sparks seen in KO cells and their elevated peak $[Ca^{2+}]_i$ levels are also reduced to WT levels by equalizing the SR Ca^{2+} content of the KO cell to that of the WT cell. These results consequently not only show how PLB modulates E–C coupling but also reveal the exquisitely important role of SR Ca^{2+} load in regulating E–C coupling. This is the first report to demonstrate this regulatory function of SR Ca^{2+} load in E–C coupling as predicted by Niggli & Lederer (1990).

Local $[Ca^{2+}]_i$ accelerates the rate of decay of I_{Ca}

Multiple processes, including $[Ca^{2+}]_i$, contribute to the inactivation of I_{Ca} (Kass & Sanguinetti, 1984; McDonald *et al.* 1994; Sham, Cleemann & Morad, 1995; Adachi- Akahane, Cleemann & Morad, 1996; Grantham & Cannell, 1996; You, Pelzer & Pelzer, 1997). We found that I_{Ca} inactivated faster in KO cells than in WT cells, an observation also made in a recent preliminary report (Masaki, Sato, Luo, Kranias & Yatani, 1996). In addition Ca^{2+} sparks in KO cells were of larger amplitude than those in WT cells, which led us to hypothesize that the increased local $[Ca^{2+}]_i$ produced by the larger Ca^{2+} sparks in KO cells was responsible for speeding up the decay of I_{Ca} in KO cells. Interestingly, we found 'normal' I_{Ca} inactivation kinetics in KO′ cells (i.e. similar to WT), when the SR Ca^{2+} content of both cell types was equal. It was under this condition that the size of elementary SR Ca^{2+} release events (i.e. Ca^{2+} sparks) in KO′ cells became equal to that in WT cells. Taken together these results show that the amplitude of the local SR Ca^{2+} signal during E–C coupling is an important determinant of the rate of inactivation of I_{Ca} as suggested by Sham *et al.* (1995) and Adachi-Akahane *et al.* (1996).

Variable rate of Ca^{2+} pumping by the SR Ca^{2+}-ATPase depends on SR Ca^{2+} load

A Ca^{2+} spark declines because, after the RyRs close, (1) Ca^{2+} diffuses from the release site to other regions of the cell with lower $[Ca^{2+}]_i$ and (2) because Ca^{2+} is taken back into the SR via the SR Ca^{2+}-ATPase (Gómez *et al.* 1996). We found that when the SR Ca^{2+} load is the same, as it is in KO′ and WT cells, Ca^{2+} sparks decline faster in KO′ than in WT cells. We attribute this to the faster turnover rate of the Ca^{2+}-ATPase in KO′ cells. When the SR Ca^{2+} load increases, however, the efficacy of pumping by the SR Ca^{2+}-ATPase declines, as would be expected if the chemical gradient across the SR membrane had measurable effects on the kinetics of Ca^{2+}-ATPase function. The larger Ca^{2+} gradient from the SR lumen to the cytosol of KO cells than of KO′ cells tends to oppose the net movement of Ca^{2+} by the Ca^{2+}-ATPase. This larger Ca^{2+} gradient is thus associated with a slower rate of pumping by the SR Ca^{2+}-ATPase, which produces Ca^{2+} sparks and global $[Ca^{2+}]_i$ transients that decline more slowly in KO cells than in KO′ cells.

The analysis of the kinetics of decay of the Ca^{2+} spark and the kinetics of decay of the cell-wide $[Ca^{2+}]_i$ transient provides important information on how the SR Ca^{2+}-ATPase contributes to these distinct Ca^{2+} signals. The less prominent role of the SR Ca^{2+}-ATPase in speeding up the decline of the Ca^{2+} spark *versus* the global $[Ca^{2+}]_i$ transient supports the conclusion that another factor (i.e. diffusion of Ca^{2+} away from its point source) dominates the decaying phase of the Ca^{2+} spark (Gómez *et al.* 1996). In contrast, the Ca^{2+}-ATPase re-uptake dominates the declining phase of the global $[Ca^{2+}]_i$ transient.

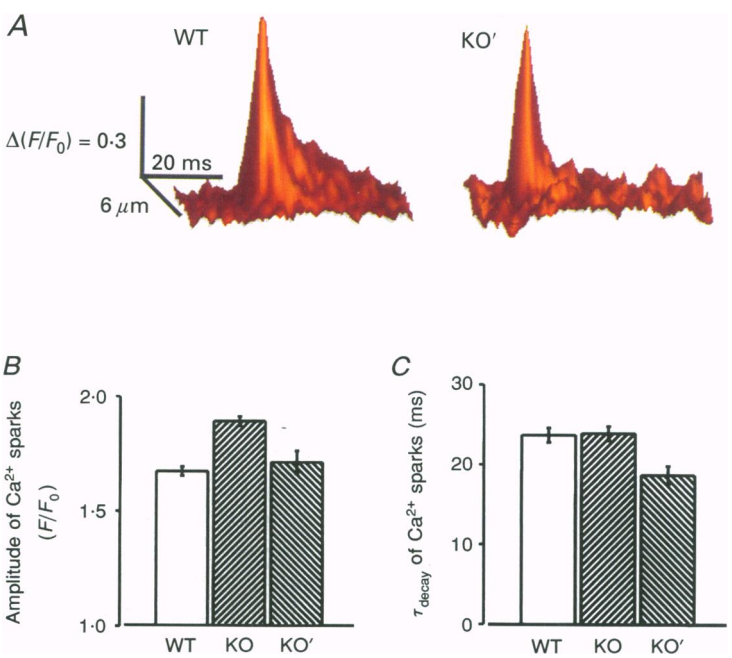

Figure 4. Effects of SR Ca^{2+} load on Ca^{2+} sparks

A, surface plot of averaged Ca^{2+} sparks from WT (left; $n = 116$ Ca^{2+} sparks from 7 animals) and KO′ (right; $n = 39$ sparks from 3 animals) myocytes. Vertical scale bar represents a fluorescence change of 0·3 in F/F_0, where the baseline $F/F_0 = 1$. *B*, amplitude of spontaneous Ca^{2+} sparks in WT, KO and KO′ ventricular myocytes. *C*, time constant of decay (τ_{decay}) of Ca^{2+} sparks in WT, KO and KO′ ventricular myocytes. WT and KO data shown in the figure are taken from Fig. 3.

Sensitivity of the RyR to triggering by local $[Ca^{2+}]_i$

β-Adrenergic stimulation increases the sensitivity of the RyR to activation by $[Ca^{2+}]_i$ by phosphorylating the RyR (Valdivia, Kaplan, Ellis-Davies & Lederer, 1995) and also phosphorylates PLB to increase the turnover rate of the SR Ca^{2+}-ATPase. We show here that, when the SR Ca^{2+}-ATPase turnover rate is increased by PLB deficiency, the sensitivity of the RyR to activation by $[Ca^{2+}]_i$ is also increased. This conclusion is based on the increase in sensitivity to $[Ca^{2+}]_i$ of spontaneous SR Ca^{2+} release (i.e. spontaneous Ca^{2+} sparks), and the augmented sensitivity to the local $[Ca^{2+}]_i$ from I_{Ca} that triggered SR Ca^{2+} release (measured as the E–C coupling gain function – see discussion below). The distinction then is that the direct action of PKA on the RyRs is augmented by increased Ca^{2+} influx through L-type Ca^{2+} channels and also by increased SR Ca^{2+} load while in KO cells only increased SR Ca^{2+} load is produced. This does, however, provide compelling evidence that an increase in the SR Ca^{2+} content alone is enough to augment the sensitivity of RyRs to $[Ca^{2+}]_i$.

The measure of E–C coupling gain used here reports the size of the $[Ca^{2+}]_i$ transient normalized to the peak I_{Ca}. Another useful measurement of E–C coupling gain would be $(d[Ca^{2+}]_i/dt)_{max}$ (a measure of the rate of SR Ca^{2+} release) divided by the peak I_{Ca}. This latter measure is more susceptible to measurement noise, especially at low levels of SR Ca^{2+} release but may provide a better measure of the relationship between the trigger (I_{Ca}) and the response (rate of SR Ca^{2+} release). In this paper we prefer to use the former measure because it appears to provide similar results and is very robust.

It has also been shown that when SR Ca^{2+} overload is produced (Cheng *et al.* 1996), Ca^{2+} sparks occur with increased frequency but in the case of SR Ca^{2+} overload, propagating waves of elevated $[Ca^{2+}]_i$ are also a dominant feature. Although KO cells do have increased SR Ca^{2+} load, as do the 'Ca^{2+} overloaded' heart cells, propagating waves of elevated $[Ca^{2+}]_i$ are not normally seen in quiescent KO cells (nor are $[Ca^{2+}]_i$ waves found in KO′ or WT cells). The effect of the increased sensitivity of the RyR to activation by $[Ca^{2+}]_i$ and the higher local $[Ca^{2+}]_i$ produced by Ca^{2+} sparks are presumably graded with respect to their ability to activate nearby SR Ca^{2+} release sites (i.e. activate nearby Ca^{2+} sparks in a regenerative process). The same argument clearly applies to the effects of β-adrenergic stimulation, which is normally not associated with the regenerative propagation of $[Ca^{2+}]_i$ waves. We conclude from this that the alteration of RyR sensitivity to $[Ca^{2+}]_i$ (produced by variations in SR Ca^{2+} load) is an important factor regulating the $[Ca^{2+}]_i$ transient and contractility and that PLB contributes to this regulation under physiological conditions.

Adachi-Akahane, S., Cleemann, L. & Morad, M. (1996). Cross-signaling between L-type Ca^{2+} channels and ryanodine receptors in rat ventricular myocytes. *Journal of General Physiology* **108**, 435–454.

Balke, C. W., Egan, T. M. & Wier, W. G. (1994). Processes that remove calcium from the cytoplasm during excitation–contraction coupling in intact rat heart cells. *Journal of Physiology* **474**, 447–462.

Bassani, J. W., Yuan, W. & Bers, D. M. (1995). Fractional SR Ca^{2+} release is regulated by trigger Ca^{2+} and SR Ca^{2+} content in cardiac myocytes. *American Journal of Physiology* **268**, C1313–1319.

Berlin, J. R. & Konishi, M. (1993). Ca^{2+} transients in cardiac myocytes measured with high and low affinity Ca^{2+} indicators. *Biophysical Journal* **65**, 1632–1647.

Cannell, M. B., Cheng, H. & Lederer, W. J. (1994). Spatial non-uniformities in $[Ca^{2+}]_i$ during excitation-contraction coupling in cardiac myocytes. *Biophysical Journal* **67**, 1942–1956.

Cannell, M. B., Cheng, H. & Lederer, W. J. (1995). The control of calcium release in heart muscle. *Science* **268**, 1045–1049.

Cheng, H., Cannell, M. B. & Lederer, W. J. (1994). Propagation of excitation-contraction coupling into ventricular myocytes. *Pflügers Archiv* **428**, 415–417.

Cheng, H., Lederer, M. R., Lederer, W. J. & Cannell, M. B. (1996). Calcium sparks and $[Ca^{2+}]_i$ waves in cardiac myocytes. *American Journal of Physiology* **270**, C148–159.

Cheng, H., Lederer, W. J. & Cannell, M. B. (1993). Calcium sparks: elementary events underlying excitation-contraction coupling in heart muscle. *Science* **262**, 740–744.

Chu, G., Luo, W., Slack, J. P., Tilgmann, C., Sweet, W. E., Spindler, M., Saupe, K. W., Boivin, G. P., Moravec, C. S., Matlib, M. A., Grupp, I. L., Ingwall, J. S. & Kranias, E. G. (1996). Compensatory mechanisms associated with the hyperdynamic function of phospholamban-deficient mouse hearts. *Circulation Research* **78**, 1064–1076.

Crespo, L. M., Grantham, C. J. & Cannell, M. B. (1990). Kinetics, stoichiometry and role of the Na^+-Ca^{2+} exchange mechanism in isolated cardiac myocytes. *Nature* **345**, 618–621.

Fabiato, A. (1983). Calcium-induced release of calcium from the cardiac sarcoplasmic reticulum. *American Journal of Physiology* **245**, C1–14.

Gómez, A. M., Cheng, H. P., Lederer, W. J. & Bers, D. M. (1996). Ca^{2+} diffusion and sarcoplasmic reticulum transport both contribute to $[Ca^{2+}]_i$ decline during Ca^{2+} sparks in rat ventricular myocytes. *Journal of Physiology* **462**, 575–581.

Grantham, C. J. & Cannell, M. B. (1996). Ca^{2+} influx during the cardiac action potential in guinea pigs ventricular myocytes. *Circulation Research* **79**, 194–200.

Hicks, M. J., Shigekawa, M. & Katz, A. M. (1979). Mechanism by which cyclic adenosine 3′:5′-monophosphate-dependent protein kinase stimulates calcium transport in cardiac sarcoplasmic reticulum. *Circulation Research* **44**, 384–391.

Kass, R. S. & Sanguinetti, M. C. (1984). Inactivation of calcium channel current in the calf Purkinje fiber. Evidence for voltage- and calcium-mediated mechanisms. *Journal of General Physiology* **84**, 705–726.

Kirby, M. S., Sagara, Y., Gaa, S., Inesi, G., Lederer, W. J. & Rogers, T. B. (1992). Thapsigargin inhibits contraction and Ca^{2+} transient in cardiac cells by specific inhibition of the sarcoplasmic reticulum Ca^{2+} pump. *Journal of Biological Chemistry* **267**, 12545–12551.

Kiss, E., Ball, N. A., Kranias, E. G. & Walsh, R. A. (1995). Differential changes in cardiac phospholamban and sarcoplasmic reticular Ca^{2+}-ATPase protein levels. *Circulation Research* **77**, 759–764.

Leblanc, N. & Hume, J. R. (1990). Sodium current-induced release of calcium from cardiac sarcoplasmic reticulum. *Science* **248**, 372–376.

Levi, A. J., Spitzer, K. W., Kohmoto, O. & Bridge, J. H. (1994). Depolarization-induced Ca entry via Na^+-Ca^{2+} exchange triggers SR release in guinea pig cardiac myocytes. *American Journal of Physiology* **266**, H1422–1433.

Lindemann, J. P., Jones, L. R., Hathaway, D. R., Henry, B. G. & Watanabe, A. M. (1983). β-Adrenergic stimulation of phospholamban phosphorylation and Ca^{2+}-ATPase activity in guinea pig ventricles. *Journal of Biological Chemistry* **258**, 464–471.

Lipp, P. & Niggli, E. (1994). Sodium current-induced calcium signals in isolated guinea-pig ventricular myocytes. *Journal of Physiology* **474**, 439–446.

López-López, J. R., Shacklock, P. S., Balke, C. W. & Wier, W. G. (1995). Local calcium transients triggered by single L-type calcium channel currents in cardiac cells. *Science* **268**, 1042–1045.

Luo, W., Grupp, I. L., Harrer, J., Ponniah, S., Grupp, G., Duffy, J. J., Doetschman, T. & Kranias, E. G. (1994). Targeted ablation of the phospholamban gene is associated with markedly enhanced myocardial contractility and loss of beta-agonist stimulation. *Circulation Research* **75**, 401–409.

Luo, W., Wolska, B. M., Grupp, I. L., Harrer, J. M., Haghighi, K., Ferguson, D. G., Slack, J. P., Grupp, G., Doetschman, T., Solaro, R. J. & Kranias, E. G. (1996). Phospholamban gene dosage effects in the mammalian heart. *Circulation Research* **79**, 839–847.

Masaki, H., Sato, Y., Luo, W., Kranias, E. G. & Yatani, A. (1996). Characteristics of L-type Ca^{2+} channel and β-adrenergic stimulation in wild-type and phospholamban-deficient mouse cardiac myocytes. *Journal of Molecular and Cellular Cardiology* **28**, A120.

McDonald, T. F., Pelzer, S., Trautwein, W. & Pelzer, D. J. (1994). Regulation and modulation of calcium channels in cardiac, skeletal, and smooth muscle cells. *Physiological Reviews* **74**, 365–507.

Niggli, E. & Lederer, W. J. (1990). Voltage-independent calcium release in heart muscle. *Science* **250**, 565–568.

Powell, T., Noma, A., Shioya, T. & Kozlowski, R. Z. (1993). Turnover rate of the cardiac Na^+–Ca^{2+} exchanger in guinea-pig ventricular myocytes. *Journal of Physiology* **472**, 45–53.

Santana, L. F., Cheng, H., Gómez, A. M., Cannell, M. B. & Lederer, W. J. (1996). Relation between the sarcolemmal Ca^{2+} current and Ca^{2+} sparks and local control theories for cardiac excitation-contraction coupling. *Circulation Research* **78**, 166–171.

Santana, L. F., Shioya, T., Kranias, E. G. & Lederer, W. J. (1997). Ca^{2+} sparks and EC coupling in phospholamban-deficient ventricular myocytes. *Biophysical Journal* **72**, A43.

Sham, J. S., Cleemann, L. & Morad, M. (1995). Functional coupling of Ca^{2+} channels and ryanodine receptors in cardiac myocytes. *Proceedings of the National Academy of Sciences of the USA* **92**, 121–125.

Simmerman, H. K., Collins, J. H., Theibert, J. L., Wegener, A. D. & Jones, L. R. (1986). Sequence analysis of phospholamban: identification of phosphorylation sites and two major structural domains. *Journal of Biological Chemistry* **261**, 13333–13341.

Talosi, L., Edes, I. & Kranias, E. G. (1993). Intracellular mechanisms mediating reversal of β-adrenergic stimulation in intact beating hearts. *American Journal of Physiology* **264**, H791–797.

Valdivia, H. H., Kaplan, J. H., Ellis-Davies, G. C. & Lederer, W. J. (1995). Rapid adaptation of cardiac ryanodine receptors: modulation by Mg^{2+} and phosphorylation. *Science* **267**, 1997–2000.

Wegener, A. D., Simmerman, H. K., Lindemann, J. P. & Jones, L. R. (1989). Phospholamban phosphorylation in intact ventricles: phosphorylation of serine 16 and threonine 17 in response to β-adrenergic stimulation. *Journal of Biological Chemistry* **264**, 11468–11474.

Wolska, B. M., Stojanovic, M. O., Luo, W., Kranias, E. G. & Solaro, R. J. (1996). Effect of ablation of phospholamban on dynamics of cardiac myocyte contraction and intracellular calcium under basal conditions and beta-adrenergic stimulation. *American Journal of Physiology* **271**, H391–397.

You, Y., Pelzer, D. J. & Pelzer, S. (1997). Modulation of L-type Ca^{2+} current by fast and slow Ca^{2+} buffering in guinea pig ventricular cardiomyocytes. *Biophysical Journal* **72**, 175–187.

Zar, J. H. (1984). *Biostatistical Analysis.* Prentice-Hall Inc., Englewood Cliffs, New Jersey.

Acknowledgements

This work was supported by grants GM14715, HL25679, HL36974, HL26057, HL22619 and HL52318. We want to thank Dr T. Shioya, a fellow of the Maryland Affiliate of the American Heart Association, for his invaluable help in the isolation of mouse ventricular myocytes.

Received 13 February 1997; accepted 15 May 1997.